Statistical Mechanics of Phase Diagrams. I. Inverse Power Potentials and the Close-Packed to Body-Centered Cubic Transition*

WILLIAM G. HOOVER

Lawrence Livermore Laboratory, Department of Applied Science, University of California at Davis-Livermore, Livermore, California 94550

AND

DAVID A. YOUNG AND RICHARD GROVER

Lawrence Livermore Laboratory, Livermore, California 94550

Most of the softer metals exhibit a low-temperature close-packed phase, an intermediate-temperature body-centered phase, and a high-temperature fluid phase. Here we relate this behavior to that of theoretical model systems in which particles interact with the inverse power potential $\phi(r) = \epsilon(\sigma/r)^n$. We show that the same three-phase behavior occurs for the models provided that the interparticle repulsion is sufficiently soft ($n \leq 7$). For the model systems the phase boundary between the close-packed and the body-centered phases is located using lattice dynamics. The fluid–solid melting line is deduced from Monte Carlo computer experiments.

Statistical mechanics supplies the link between the microscopic world of interparticle forces and the gross thermodynamic description of pressure, volume, and temperature measurements. A comparison of statistical calculations with experimental results can furnish correlations between thermodynamic quantities and the underlying microscopic forces. Such correlations are most nearly complete for the simplest of materials, the rare gases. These gases can be understood in quantitative detail in terms of a steep repulsive force coupled with a weak van der Waals attraction. Such a theoretical model explains the existence of the triple point, where liquid, solid, and gas coexist; the gas–liquid critical point; and the melting line linking the fluid phases with a close-packed solid phase.[1]

In the present series of papers we want to consider materials more complicated than the rare gases. In describing the thermodynamics of more complicated systems, such as the metallic elements, one first of all determines the gross features of each material's behavior. What thermodynamic phases are found, as functions of temperature and pressure? The answer is conventionally displayed in a *Phase Diagram* dividing up the pressure–temperature plane into the separate regions occupied by the various phases and their combinations.[2] The most common feature of experimental phase diagrams is melting. Nearly all materials melt and freeze. The early computer experiments[3] verified Bridgman's suggestion that the ordering induced by repulsive molecular cores is responsible for the freezing transition.[4] More recent computer studies have shown that the melting transition is strikingly insensitive to the steepness of the repulsive forces.[5]

In real phase diagrams the solid region is much more complicated than that of the idealized hard-sphere model. Typically *several* different solid phases with different crystal structures exist. Despite this apparent complexity a simple macroscopic approach in which the Gibbs free energy differences between the various pairs of phases are assumed linear in pressure and temperature can semiquantitatively reproduce the

phase diagrams of the transition metals and their mixtures.[6] The success of this macroscopic approach suggests that a relatively simple *microscopic* theory should be capable of yielding realistic phase diagrams together with the insight that a microscopic interpretation adds.

The present paper is devoted to a theoretical study of the polymorphic transition from a close-packed (cp) to a body-centered cubic (bcc) solid. Next to melting itself this transition is probably the one most commonly displayed by simple metals. The first column of Table I lists the 22 metals known to exhibit the polymorphic transition cp→bcc at atmospheric pressure. The transition temperature, relative to the melting temperature, is displayed for the same 22 metals in Fig. 1.

The fact that so many metals show the close-packed to body-centered transition suggests that many simple theoretical models should show it too. We choose the simplest such model, basing our calculations on the inverse power potential

$$\phi(r) = \epsilon(\sigma/r)^n. \tag{1}$$

For this potential a single isotherm, isochore, or isobar can be used to determine the entire phase diagram.[5] Our solid-phase calculations are based on the simplifying microscopic assumption that the forces between pairs of interacting particles are linear in the particle separations. This is the quasiharmonic approximation of lattice dynamics.

Before lattice dynamics can be applied to any crystal structure that structure must be mechanically stable. For a cubic crystal under a hydrostatic pressure P this means that the isothermal and adiabatic bulk moduli, together with the two independent shear moduli, $(C_{44} - P)$ and $(C_{11} - C_{12} - 2P)/2$, must all be positive.[7] For inverse power potentials *all* of the many close-packed phases (face-centered cubic, hexagonal close packed, Samarium, double hcp, ···) satisfy the mechanical stability tests. Because the properties of the various close packings are so similar we consider

TABLE I. Values of the Grüneisen $\gamma \equiv V(\partial P/\partial E)_v$ for metallic solids grouped according to phases stable at atmospheric pressure. Except for more recent values from R. Grover, J. Phys. Chem. Solids **32**, 2539 (1971) for sodium and rubidium the γ values are those tabulated by K. A. Gschneidner, Jr., Solid State Phys. **16**, 275 (1964).

cp→bcc		cp		bcc	
Be	1.2	Cu	2.0	Li	0.9
Ca	1.0	Ag	2.4	Na	1.2
Sr	0.9	Au	3.1	K	1.3
Sc	1.0			Rb	1.4
Y	1.0	Mg	1.6	Cs	1.4
Tl	2.2	Al	2.1	Eu	1.6
		Zn	2.0		
Ti	1.3	Cd	2.3	Ba	0.9
Zr	0.7	Pb	2.7		
Hf	1.0			V	1.4
Th	1.3	Co	2.0	Cr	1.5
Mn	1.2	Ni	1.8	Nb	1.6
Fe	1.7	Tc	2.6	Mo	1.6
		Ru	3.1	Ta	1.7
La	0.7	Rh	2.3	W	1.8
Ce	0.5	Pd	2.2		
Pr	0.5	Re	2.6		
Nd	0.7	Os	2.0		
Sm	0.6	Ir	2.4		
Gd	0.5	Pt	2.7		
Tb	0.8				
Dy	0.8	Er	1.0		
Ho	0.9	Tm	1.1		
Yb	1.0	Lu	0.7		

here only the face-centered cubic phase as typical of the whole group. The thermodynamic properties for a face-centered crystal composed of inverse power particles have already been calculated and tabulated.[5]

The mechanical stability of the body-centered-cubic inverse power crystals has not been previously studied. It is easily established, by adding up known lattice

FIG. 1. The temperature range over which the body-centered phase is stable at atmospheric pressure is indicated for 22 metals as a function of the atomic number Z.

sums[8] that perfect (no thermal or zero-point motion) body-centered crystals composed of particles interacting with a sufficiently soft repulsion $(n \leq 7)$ are mechanically stable. For steeper repulsion the body-centered-cubic structure is unstable to shear. The modulus indicating this instability is $(C_{11}-C_{12}-2P)/2$. That shear modulus is negative for n equal to eight or more.
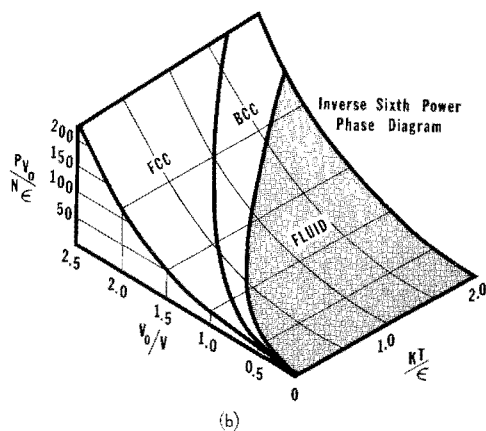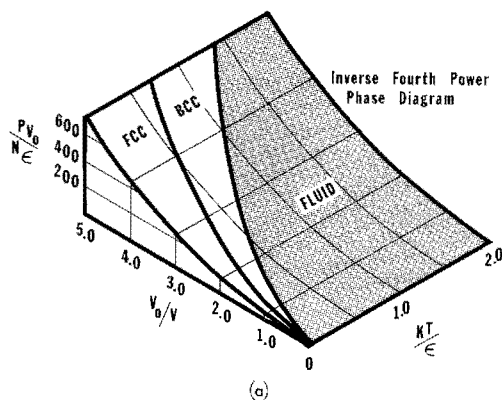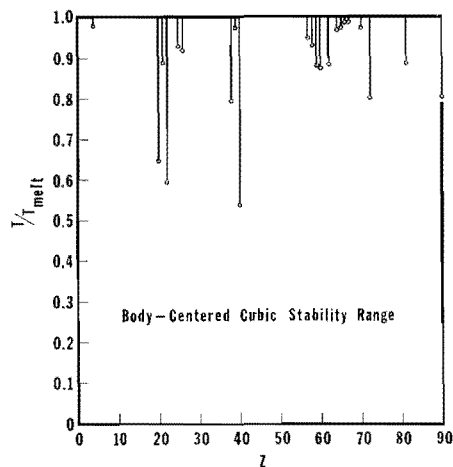

FIG. 2. Phase diagrams for systems composed of particles interacting with repulsive inverse fourth-power and inverse sixth-power pair potentials. The regions in which the fluid, bcc, and fcc phases are stable are shown. The volume V_0 is $N\sigma^3/\sqrt{2}$.

Because both the close-packed and body-centered-cubic forms are mechanically stable for the softer inverse powers it is possible that a thermodynamic transition occurs linking the two forms. The body-centered structure, with only eight nearest neighbors and six close-in second neighbors, is more loosely packed than the face-centered structure. Hard spheres packed into the body-centered arrangement would have a density 9% less than when close packed. The looser packing means that the body-centered crystal has relatively many low-frequency shear modes. These large-amplitude vibrations tend to increase the body-centered vibrational entropy relative to that of the close-packed form.[9] If the resulting entropy difference is large enough, then the higher-energy body-centered form can be stabilized with a lower *free* energy than the competing close-packed form.

TABLE II. Quasiharmonic properties for N-particle body-centered-cubic crystals. The entropy relative to the Einstein model prediction $\Delta S/Nk \equiv C(N) \equiv (1/N) \sum \ln(\nu_E/\nu)$ and the mean-squared displacement relative to the Einstein model prediction $(3N-3)^{-1}\sum(\nu_E/\nu)^2$ are tabulated for various periodic crystals. The particles interact with pairwise-additive inverse fourth- or sixth-power potentials. The Einstein frequencies ν_E are tabulated along with extrapolated values for infinite crystals. The corresponding numbers for face-centered crystals (fcc) are taken from Ref. 5. The reduced density ρ is $(N/V)\sigma^3/\sqrt{2}$.

N	$\phi(r) = \epsilon(\sigma/r)^4$			$\phi(r) = \epsilon(\sigma/r)^6$		
	$C(N)$	$\langle(\delta r/\delta r_E)^2\rangle$	$\nu_E\sigma(m/\epsilon)^{1/2}/\rho$	$C(N)$	$\langle(\delta r/\delta r_E)^2\rangle$	$\nu_E\sigma(m/\epsilon)^{1/2}/\rho^{4/3}$
2	−0.51986	0.500	0.3465	−0.51986	0.500	0.5637
16	Unstable		1.0647	Unstable		1.6921
54	Unstable		1.1781	+0.96250	105.126	1.8034
128	Unstable		1.1990	0.62961	7.091	1.8115
250	Unstable		1.2060	0.60437	5.435	1.8131
432	+0.65203	9.298	1.2090	0.59706	4.890	1.8135
686	0.63241	5.497	1.2105	0.59417	4.609	1.8137
1024	0.62519	4.572	1.2114	0.59287	4.437	1.8137
1458	0.62174	4.171	1.2119	0.59225	4.320	1.8138
2000	0.61987	3.955	1.2122	0.59196	4.236	1.8138
2662	0.61878	3.823	1.2124	0.59182	4.173	1.8138
3456	0.61810	3.736	1.2126	0.59177	4.124	1.8138
4394	0.61766	3.676	1.2127	0.59176	4.085	1.8138
5488	0.61736	3.632	1.2127	0.59176	4.053	1.8138
6750	0.61715	3.599	1.2128	0.59178	4.026	1.8138
8192	0.61700	3.574	1.2128	0.59181	4.004	1.8138
∞	0.6164	3.46	1.2130	0.5920	3.89	1.8138
fcc	0.5127	2.63	1.2102	0.4370	2.32	1.8008

To find out whether the lower frequencies from the looser packing do stabilize the body-centered-cubic crystals we carried out a series of numerical free energy calculations for inverse fourth and sixth power potentials. The detailed results are summarized in Table II. Note that the body-centered entropy exceeds that predicted by the one-particle Einstein approximation. The excess, $0.6164Nk$ in the fourth-power case and $0.5920Nk$ in the sixth-power case, is larger than that found for the corresponding face-centered crystals[5] ($0.5127Nk$ and $0.4370Nk$, respectively). The lower frequencies do indeed stabilize the body-centered form. The mean squared displacement of particles in the crystal relative to the Einstein model prediction also indicates the effect of the looser body-centered packing. The data in Table II show a 30%–40% increase in mean squared displacement on going from the face-centered to the body-centered packing at fixed density and temperature.

To compare the free energies of the face-centered and body-centered crystals we need to take into account the relatively small differences between the Einstein-model Helmholtz free energies:

$$(A_{bcc}^E - A_{fcc}^E) = 0.0078N\epsilon\rho^{4/3} + 0.0069NkT,$$

$$\text{for } n=4,$$

$$(A_{bcc}^E - A_{fcc}^E) = 0.0343N\epsilon\rho^2 + 0.0216NkT,$$

$$\text{for } n=6.$$

The dimensionless density ρ is $(N/V)\sigma^3/\sqrt{2}$. The Helmholtz free energy comparison shows that the body-centered and face-centered crystals have equal Helmholtz free energies at

$$kT/\epsilon = 0.080\rho^{4/3}, \quad \text{for } n=4;$$

$$kT/\epsilon = 0.257\rho^2, \quad \text{for } n=6.$$

Because these transition temperatures lie well below the melting temperatures, $0.161\rho^{4/3}\epsilon/k$ and $0.411\rho^2\epsilon/k$ it seems likely that the polymorphic transitions indicated by the quasiharmonic approximation actually do occur. If the cell model is used to estimate anharmonic corrections to the quasiharmonic predictions, the results are found to be insensitive to crystal structure. The quasiharmonic free energy *differences* should therefore be accurate.

For the melting transition bcc→fluid the quasiharmonic free energies are probably less accurate. We continue to use the melting line determined earlier for the face-centered phase,[4] expecting that the fusion properties of the body-centered and face-centered phases are similar.

The PVT phase diagrams resulting from our calculations are shown in Fig. 2. The lack of attractive forces to provide the cohesive energy and liquid phase characteristic of real metals is evident. The diagrams do show the three-phase behavior characteristic of soft metals at atmospheric pressure.

How can we correlate the theoretical results with experiment? The metals are divided into three separate classes in Table I. Those which show the transition cp→bcc, those which remain close packed at all temperatures, and those which remain body centered at all temperatures. (The classification is based on atmospheric pressure data.) Although the metals showing the transition are by and large softer than the others, values of the bulk moduli vary erratically through all three groups. Many of the metals showing the transition are actually harder than representatives of the close-packed group. Another possible way of classifying the experimental metals' softness is through the Grüneisen gamma

$$\gamma \equiv V(\partial p/\partial E)_v. \qquad (2)$$

This thermodynamic quantity depends, for quasiharmonic crystals, on the third derivative of the potential, and thus it emphasizes the repulsive forces idealized in our inverse power models. For a quasiharmonic crystal the relation between γ and n is $\gamma = (n+2)/6$. Table I shows that the values do furnish a reliable dividing line between the first two columns. The metals showing the transition (except for Thallium) have maximum γ values of 1.7 (corresponding to $n=8$). The close-packed materials not showing the transition have mostly larger γ values. Thus the critical γ value of 1.7, separating real metals showing the transition from those not showing it, is nearly the same as the critical value 1.5 predicted by our theoretical lattice dynamics work based on inverse power potentials.

To avoid leaving the impression that this similarity between the γ dependence of inverse power polymorphic transitions and the γ dependence of real metal polymorphic transitions implies complete correlation of the phase diagrams, we point out several features requiring a somewhat more complicated explanation:

(1) Under atmospheric pressure many metals are body centered even at zero kelvins and never show the transition. These are the metals shown in the third column of Table I.

(2) The body-centered phase is, for several metals, denser than the "close-packed" phase. This is counter to the inverse power potential predictions.

(3) The temperature of the polymorphic transition, relative to the melting transition temperature, varies rather erratically, as shown in Fig. 1.

(4) The small γ values found for some metals, notably the rare earths, correspond to unphysically small values of n.

(5) The bcc phase tends to disappear at high pressure.

All five of these features are probably consistent with weak attractions which can, at low pressure, reduce γ and vary the densities and temperatures at which the two solid phases can coexist.

A sixth feature is more puzzling and deserves further

investigation: In the model systems the forces due to a great number of neighbors must be included to stabilize the body-centered form. (This follows from the rather large but still unstable crystals appearing in Table II.) In real metals our intuition suggests that a model with repulsive interactions spanning two or three shells of neighbors should provide adequate complexity for interpreting thermodynamic properties. Perhaps attractive forces can provide a partial explanation. At zero pressure the attractive forces replace the shear modulus $(C_{11}-C_{12}-2P)/2$ by $(C_{11}-C_{12})/2$. That modulus is positive if only first and second neighbors in a body-centered crystal are included. Such an explanation however, could no longer distinguish a difference in mechanical stability between the small-γ and large-γ materials. On the other hand, at very high pressures the attractions can no longer be important. The disappearance of the body-centered phase under these conditions in real metals therefore indicates that the repulsive forces in metals are not really of such long range.

We expect that the correlation found here between the Grüneisen γ and the phase diagram will serve to stimulate more detailed investigations.

ACKNOWLEDGMENTS

* Work performed under the auspices of the United States Atomic Energy Commission.

[1] J.-P. Hansen and L. Verlet, Phys. Rev. **184**, 151 (1969) have carried out detailed thermodynamic computer experiments using the Lennard-Jones–Mie potential. Calculations for a more realistic potential with three-body forces included have been carried out by John Barker and his co-workers. See M. V. Bobetic and J. A. Barker, Phys. Rev. B **2**, 4169 (1970) and J. A. Barker, M. L. Klein, and M. V. Bobetic, *ibid.* **2**, 4176 (1970).

[2] A collection of phase diagrams for many elements and some compounds appears in W. Klement and A. Jayaraman, Progr. Solid State Chem. **3**, 289 (1967).

[3] W. W. Wood, F. R. Parker, and J. D. Jacobson, Nuovo Cimento Suppl. **9**, 133 (1958); T. E. Wainwright and B. J. Alder, *ibid.* **9**, 116 (1958).

[4] P. W. Bridgman, Phys. Rev. **3**, 126, 153 (1914).

[5] W. G. Hoover, S. G. Gray, and K. W. Johnson, J. Chem. Phys. **55**, 1128 (1971).

[6] L. Kaufman and H. Bernstein, *Computer Calculation of Phase Diagrams* (Academic, New York, 1970).

[7] The elastic constants C_{ij} are used in describing the work necessary to deform a crystal using the corresponding Lagrangian strains **n**. Under isothermal conditions $VC_{ij}{}^T \equiv (\partial^2 A/\partial \eta_i \partial \eta_j)_T$; under adiabatic conditions $VC_{ij}{}^S \equiv (\partial^2 E/\partial \eta_i \partial \eta_j)_S$. The isothermal and adiabatic shear constants are equal: $C_{44}{}^S = C_{44}{}^T$ and $(C_{11}{}^S - C_{12}{}^S - 2P)/2 = (C_{11}{}^T - C_{12}{}^T - 2P)/2$; while the adiabatic bulk modulus always exceeds the isothermal one. For numerical calculations see A. C. Holt, W. G. Hoover, S. G. Gray, and D. R. Shortle, Physica **49**, 61 (1970).

[8] M. Born and R. D. Misra, Proc. Cambridge Phil. Soc. **36**, 466 (1940).

[9] C. Zener, in *Phase Stability in Metals and Alloys*, edited by P. S. Rudman, J. Stringer, and R. I. Jaffee (McGraw-Hill, New York, 1967), pp. 25–37.